Nanoscale Advances

ROYAL SOCIETY OF CHEMISTRY

PAPER

View Article Online
View Journal | View Issue

Cite this: *Nanoscale Adv.*, 2022, **4**, 2303

Synthesis of an insulin intercalated graphene oxide nanogel composite: evaluation of its release profile and stability for oral delivery of insulin

Shabana Gul Baloch, Huma Shaikh, * Shahnila Shah, Shahabuddin Memon and Ayaz Ali Memon

Diabetes mellitus (DM) is a disorder of glucose regulation produced due to insufficient availability of insulin. Generally, insulin is given to diabetes patients *via* subcutaneous injection which is a painful method to deliver this drug. In this work we have made an attempt to develop an oral drug delivery system that can efficiently deliver insulin to the small intestine. An insulin intercalated GO based nanogel composite (In@GO NgC) was fabricated for oral delivery of insulin. The *in vitro* release of insulin from In@GO NgC was studied in artificial gastric (pH 1.2) and intestinal (pH 7.5) fluids. The In@GO NgC produced better release in artificial intestinal fluid as compared to gastric fluid. The enzymatic degradation of released insulin was also examined and the results revealed that even after 6 h of incubation, the gel remained stable and the un-degraded insulin seemed to be sufficient for the physiological processes. The efficacy of In@GO NgC was also confirmed by comparing its release profile with non-intercalated GO NgC and nanogel (Ng) without GO. The prepared nanogels were thoroughly characterized using FTIR, SEM, EDS, DSC and DLS. The better release profile and enzymatic stability of In@GO NgC suggests that it can be utilized for oral drug delivery of insulin.

Received 23rd December 2021
Accepted 6th April 2022

DOI: 10.1039/d1na00887k

rsc.li/nanoscale-advances

Introduction

Diabetes mellitus (DM) is a disorder of glucose regulation produced due to insufficient availability of insulin. It is a global problem by which millions of people are affected across the world.[1,2] The International Diabetes Federation estimated that more than 366 million people were living with diabetes in the past few years and by 2030 this number is expected to increase to 522 million.[3] The common treatment for diabetes mellitus (type 1 and type 2) patients is periodic subcutaneous injection of insulin. Unlike normal insulin secretion this is an inadequate approach, therefore, a self-regulated delivery system is required to maintain blood glucose levels within the normal range.[4–9] To overcome the hyperglycemic conditions and prevention of the resulting problems in diabetic patients, it is important to produce a simple, continuous, and effective self-regulated drug delivery system.[10] Diabetic patients who rely on total insulin intake usually suffer from different problems including chronic hyperglycemia and hypoglycemia when they cannot take insulin on time.[11] However, continuous instability in blood glucose levels may cause severe cardiovascular disorders and chronic renal failure. Hypoglycemia can also cause coma and sometimes death.[12] Keeping in mind these adverse effects, various researchers have endeavored to develop a useful and safe noninvasive method for drug delivery of insulin.[13–15] However, the effectiveness of oral delivery systems for insulin has a few limitations like low absorption due to release and digestion in stomach and quick enzymatic degradation. To protect the therapeutic peptide from these enzymatic barriers, encapsulation could be used.[16,17] Encapsulation gives protection from enzymatic activity and the improved delivery system targets the colon, where the action of enzymes is relatively small.[18] The encapsulation also enhances bimolecular stability and reduces toxicity due to the controlled release mechanism. Insulin is mainly administered subcutaneously by different methods such as syringe and vial, continuous subcutaneous insulin infusion (CSII) and insulin pens. Besides, pulmonary, oral, buckle, transdermal, nasal, rectal and ocular routes of administration can also be followed.

Oral drug delivery systems with colon-specific release are presently considered as important DDS for achieving general curative goals. However, the large intestine is not ideally suited for absorption of drugs but it has some positive benefits over the small intestine such as long passage time, which prevents enzymatic degradation and is highly responsive to enhance permeation. Colon targeted insulin delivery systems administered through the oral route were formulated in accordance with micro flora, pH- and time-dependent approaches.[19] Oral delivery NDDS offers some advantages such as enhanced efficiency of the drug, targeted delivery, and reduced side effects.[20] Various drug delivery systems reported

National Centre of Excellence in Analytical Chemistry, University of Sindh, Jamshoro, Pakistan. E-mail: huma.hashu@gmail.com

for oral delivery of insulin are nanoparticles (NPs), liposomes, microemulsions (MEs) self-nano emulsifying drug delivery systems (SNEDDS), micelles, nanogels (NGs), microspheres, niosomes, and super porous hydrogels (SPHs).[21] Nanogels are aqueous dispersions of particles formed by physical or chemical cross-linking of polymeric networks of nanosized hydrogels. The physical cross-linking or self-assembly of cholesterol-modified polysaccharides results in the formation of hydrogels of nanoscale size.[22,23] Nanogels are extremely promising nano-carriers for drug delivery because they have high stability, high loading capacity, and smart responsiveness to different environmental conditions, such as temperature, pH and ionic strength, which are unusual in ordinary pharmaceutical nano-carriers.[24,25]

In this study, HEMA (hydroxyethyl methacrylate) was selected for the synthesis of the nanogel because of its characteristic low fouling nature. The emulsion polymerization method was used to overcome body circulation challenges and intestinal absorption simultaneously.[25] NIPPAM (*N*-isopropylacrylamide) was also used together with HEMA, it is stimuli responsive, also used for the thermal phase transition, to enhance or suppress charge-driven swelling transitions in glucose-responsiveness, enabling the temperature to be used as a control switch for a targeted secondary phase transition.[26] Insulin intercalated graphene oxide (In@GO) was used as a nanocarrier for insulin delivery.

In recent years, nanocomposites are explored as controlled drug delivery vehicles and have gathered more attention due to their distinctive structure and unique properties.[27] An oxidative derivative of graphene, graphene oxide (GO), has also attracted broad interest in drug delivery. The sheets of graphene oxide are enriched with hydroxyl (–OH) and epoxy (–C–O–C) groups on the basal plan and carboxylic (–COOH) and carbonyl (–CO) groups at the edges of the sheets. Thus, GO sheets with a two-dimensional plane structure and one-atom thickness can offer a large surface area to carry drugs *via* hydrogen bonding, surface adsorption, and other interactions, which make it effective as a drug nano-carrier.[28,29]

In this paper, an insulin intercalated graphene oxide nanocomposite was synthesized at first and then embedded into the pHEMA-*co*-pNIPAAM nanogel *via* emulsion polymerization. The effect of intercalation on the release patterns of In@GO NgC was studied by comparing the release patterns of GO NgC and the non-embedded nanogel (Ng).

Experimental

Chemical and reagents

2-Hydroxyethyl methacrylate (HEMA) was purchased from Daejung Chemicals & Metals, Korea. Azobisisobutyronitrile (AIBN), NIPAAM and insulin standard were purchased from Sigma-Aldrich, St. Louis, MO, USA. Tween 80 was purchased from MP biomedicals, Fischer chemicals UK and polyethylene glycol 300 (PEG) was purchased from Merk, Tokyo kasai. Pepsin and trypsin were purchased from BDH Ltd. (Poole, UK). All the chemicals and reagents were of analytical or HPLC grade.

Synthesis of graphene oxide (GO) and insulin intercalated graphene oxide nanocomposite (In@GO NC)

The graphite flakes were exfoliated into graphene oxide (GO) using the modified Hummers' method.[30] Later on, exfoliated GO was used in intercalation and the insulin intercalated GO nanocomposite (In@GO NC) was prepared by adding 0.1 g GO into 40 mL of deionized water. The dispersion was prepared using an ultrasonic bath for 30 min at ambient temperature, then 5 mg insulin standard was added into it and stirred for another 4 h. Afterwards, the mixture was washed with water to remove the extra or free insulin. The yielding insulin intercalated GO nanocomposite (In@GO NC) was dried and used in further experiments.

Synthesis of the nanogel-composite

The In@GO NgC was synthesized by the emulsion polymerization method. Briefly, 3 mL of PEG and 3 mL of Tween 80 were dissolved in 100 mL of *n*-hexane then 50 mg of the AIBN initiator was added in the solution and kept in an ice bath. 1 mL of HEMA and 20 mg of NIPAAM and well dispersed In@GO NC were dissolved in 5 mL of Tris–HCl buffer at pH = 4. Both the solutions were mixed by strong homogenization to form a micro-emulsion. The reaction was carried out at 50 °C in a water bath with continuous overnight stirring for polymerization. The In@GO NgC was first washed with hexane and then with DI water to remove the surfactants, the denatured insulin, unreacted small molecules and residual organic solvent from the nanogel. Fig. 1 illustrates the graphical representation of the synthesis of In@GO NgC. The prepared gel was finally dried and stored at 4 °C until further characterization and release studies.[25] The GO nanogel composite (GO NgC) and nanogel (Ng) were also synthesized using the same strategy. The only difference was that in the former non intercalated GO was used and in the latter GO was not used during the fabrication of the nanogels.

Characterization

FT-IR spectroscopy (Thermo Scientific Nicolet™ iS10) was used to study the functionalities of the different materials prepared. The morphological structure of the materials was detected by SEM (JSM-6491 LV, Joel, Japan). Elemental analysis was also performed by EDS. The polydispersity index (PDI) and hydrodynamic size of the nanogels were characterized by dynamic light scattering (DLS) with a Zetasizer (Malvern Instruments, Malvern, UK). The thermal stability of GO and In@GO NC was characterized by DSC (Mettler Toledo 822e). A nitrogen atmosphere was used at the flow rate of 50 mL min^{-1}. 5 mg of the dried sample was placed in an aluminum pan and samples were sealed. The samples were heated from ambient temperature to 500 °C approximately, at a heating rate of 10 °C min^{-1}.

The swelling properties of the synthesized nanogels were found by the gravimetric analytical method. The swelling behavior of the synthesized materials was examined in PBS (phosphate buffer saline) with pH 6.8, 7.4, acidic water pH 1.2, and D. I. Water. 10 mg of dried nanogel (W_0) was immersed in

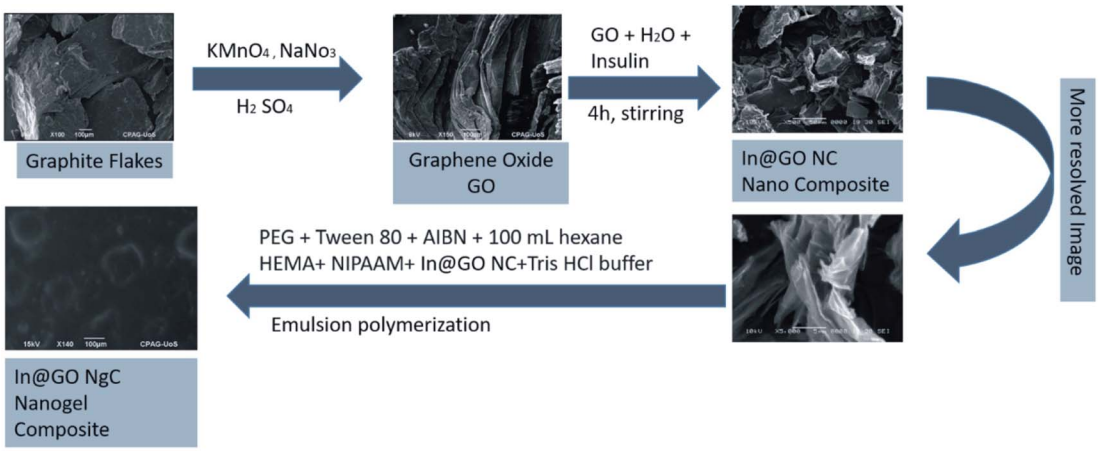

Fig. 1 Graphical representation of the synthesis of In@GO NgC.

10 mL of solvents at 37 °C. Then, the respective solvent was removed under predetermined intervals and the nanogel was weighed after removing excess solution on the surface. The swelling ratio of the nanogel was calculated using the following formula.

$$\mathrm{Sw}/w = (m_{\text{wet gel}} - m_{\text{dry gel}})/m_{\text{dry gel}}$$

$$\text{Swelling ratio} = (m_{\text{swollen gel}} - m_{\text{dried gel}})/m_{\text{swollen gel}} \times 100\%$$

The viscous behaviors of In@GO NgC, GO NgC, and Ng were analyzed by using Ostwald's viscometer. Precisely, a definite volume (12 mL) of the gel under examination was poured into the viscometer. The gel was sucked from the left-arm a little bit above the mark A. Then liquid was allowed to flow back towards mark B. The time of flow of the liquid from A to B was noted. The process was repeated three times for all the samples.

Loading efficiency

50 mg of insulin was loaded in 50 mg of In@GO NgC, GO NgC and Ng dispersed in 50 mM Tris–HCl buffer (TBS) separately. The amount of insulin before and after loading was determined using the UV-vis spectrophotometer at 214 and 270 nm. The loading efficiency (LE) was calculated by the following formula:

$$\%\ \mathrm{LE} = (M_1/M_t) \times 100$$

where % LE is the percentage loading efficiency, M_1 is the amount of insulin loaded into the gels and M_t is the total amount of insulin taken for loading into the gels.

In vitro insulin release studies

In vitro release of insulin from the synthesized nanogels, *i.e.*, In@GO NgC, GO NgC and Ng was performed using artificial gastric and intestinal fluids. 30 mg of the insulin loaded nanogel was dispersed in 10 mL of artificial gastric fluid [2.0 g L^{-1} of NaCl and 7.0 mL L^{-1} of conc. HCl in deionized water] and 10 mL of artificial intestinal fluid [50 mM Tris–HCl buffer saline (TBS) pH 7.5].[32] The sample vials were maintained at the temperature of 37 °C. At different intervals of time, the absorbance was recorded at 214 nm and 270 nm to observe the release of insulin. The concentration of insulin was determined in mg mL^{-1}.

Insulin release was calculated as follows:

$$\text{Insulin release}\% = M_t/M_{\text{in}} \times 100$$

where M_t is the amount of insulin released at time t and M_{in} is the amount of insulin in the nanogels at time $t = 0$.

In vitro release of insulin towards enzymatic fluids

50 mg of each (In@GO NgC, GO NgC and Ng) insulin loaded nanogel was placed in artificial intestinal fluid with trypsin (2 units per mL) and artificial gastric fluid with pepsin (1 unit per mL). The samples were maintained at 37 °C for 6 hours. The amount of insulin released was evaluated with intervals of 1 h using a UV/Vis spectrophotometer. The amount of remaining un-degraded insulin was calculated.[31]

Release kinetics study of nanogels for insulin

The release kinetics of nanogels for insulin was studied on a UV/Vis spectrophotometer at the wavelengths of 214 nm and 270 nm in artificial gastric and intestinal fluids of pH 1.2 and pH 7.5, respectively. Generally five kinetic models are used to investigate the drug release from various controlled release formulations and the best and more appropriate equation is evaluated for the *in vitro* release calculations.[32]

Zero order kinetics is a release system in which the drug release does not depend on the drug's concentration. The zero order release equation is given below:

$$Ft = K_0 t$$

where F is the amount of drug released at time t, while K_0 is the constant of zero-order release.[33]

First-order kinetics

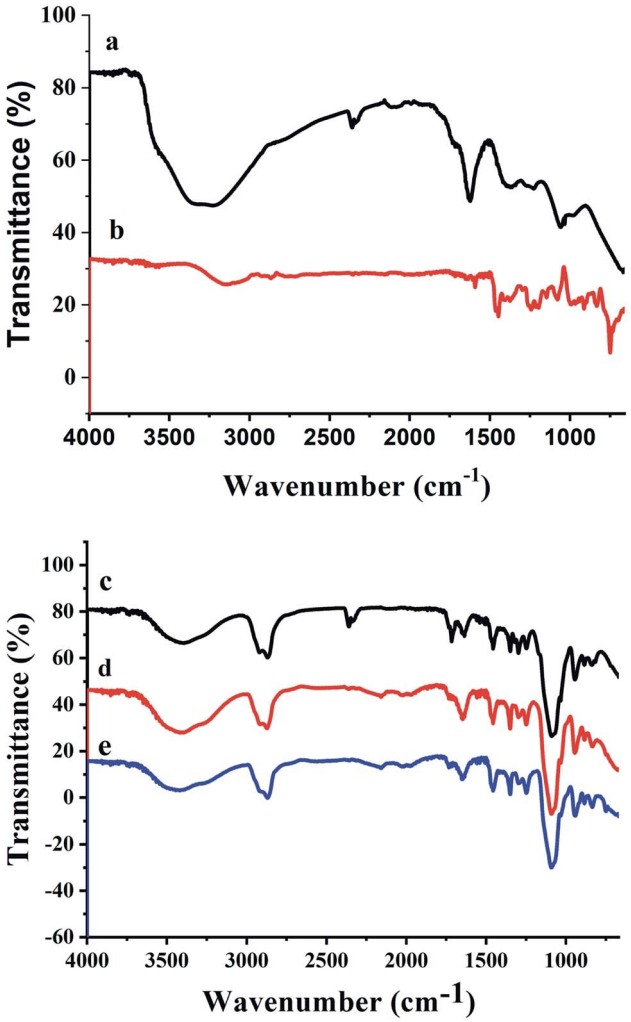

Fig. 2 FTIR spectra of (a) GO, (b) In@GO NC, (c) In@GO NgC, (d) GO NgC and (e) Ng.

$$\ln(1 - F) = -K_1 t$$

where F shows the amount of drug released at time t, while K_1 is the constant of first-order release.[34]

Higuchi kinetic model

$$F = K_2 t_{1/2}$$

where F represents the amount of the drug released at time t, while K_2 is the constant and known as the Higuchi's constant.[35]

Korsmeyer–Peppas kinetic model

$$M_t/M_\infty = K_3 t_n$$

Here M_t is the amount of drug released at time t, M_∞ is the amount of drug released at time infinity, K_3 is the kinetic constant and n is the exponent describing the swelling mechanism.

Hixson–Crowell kinetic model

$$W_0^{1/3} - W_t^{1/3} = \kappa t$$

Here W_0 is the initial amount of drug, W_t is the remaining amount of drug at time t, while κ (kappa) is a constant that shows the surface and volume relation.

Results and discussion

The synthesized nanogels were thoroughly characterized using different characterization techniques. The chemical composition was studied using FTIR spectroscopy. The FTIR spectrum of GO (Fig. 2a) shows the stretching bands at 3278 cm^{-1} due to O–H stretching from hydroxyl and carboxylic acid functionalities. Stretching bands at 1621 cm^{-1} and 1059 cm^{-1} confirmed the presence of oxygen containing functionalities such as carboxyl, epoxy and hydroxyl groups in GO.[36] While the intercalation of insulin with GO in Fig. 2b shows that the

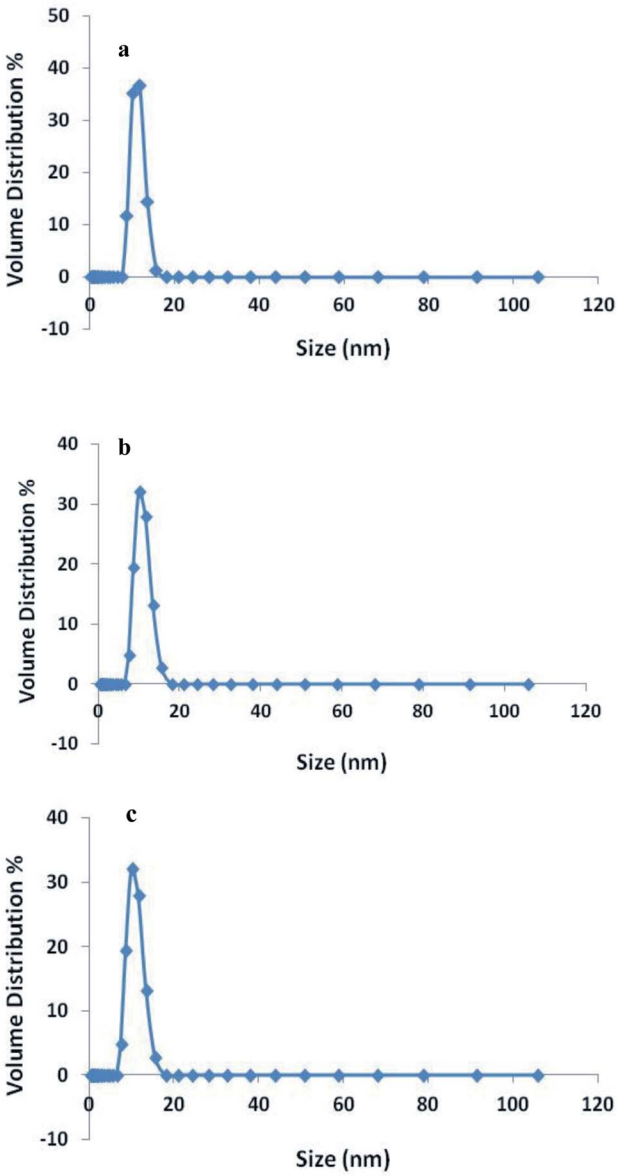

Fig. 3 Particle size of nanogels through DLS (a) IN@GO NgC (b) GO NgC and (c) Ng.

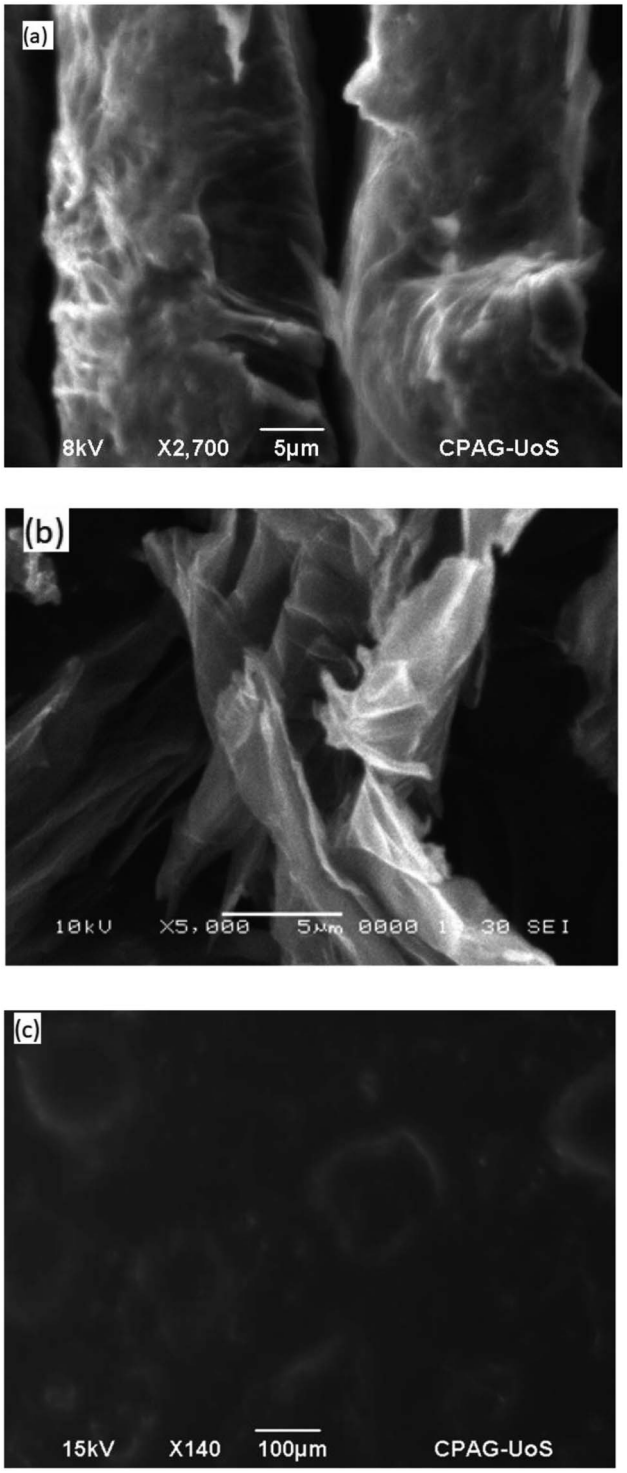

Fig. 4 SEM images of (a) GO (b) In@GO NC and (c) In@GO NgC.

characteristic peak of O–H stretching from hydroxyl groups at 3278 cm^{-1} in GO has been shifted to 3146 cm^{-1} in In@GO NC. The peak at 1590 cm^{-1} due to C–N bending reveals the presence of the amine due to insulin which confirms the interaction of GO with the insulin.

The FTIR spectra of In@GO NgC, GO NgC, and Ng are given in Fig. 2c, d and e, respectively. These three spectra showed characteristic bands in the range of 400–4000 cm^{-1}. A band of stretching in the range of 3200–3600 cm^{-1} corresponds to the hydroxyl group (–OH); another band in the range of 2847–2948 cm^{-1} is attributed to stretching of methyl ($–CH_3$) and methylene ($–CH_2–$) groups; a stretching band between 1636–1646.90 cm^{-1} is related to the ester carboxyl groups (C═O); while the band at 1451 cm^{-1} is related to the –CH bending.[37,38] The stretching bands at 1247 cm^{-1}, 1297 cm^{-1}, 1348 cm^{-1}, and 1456 cm^{-1} are due to C–N and –OH moieties. An intense peak in the region of 1089–1092 cm^{-1} is shown in all three spectra, which represents the –C–N stretching. The FTIR spectra of synthesized nanogels show that the polymerization has been achieved successfully.[25,39]

The size of the synthesized nanogels was characterized by DLS and the results are shown in Fig. 3. The DLS studies showed that the hydrodynamic size of In@GO NgC was 11.10 nm in

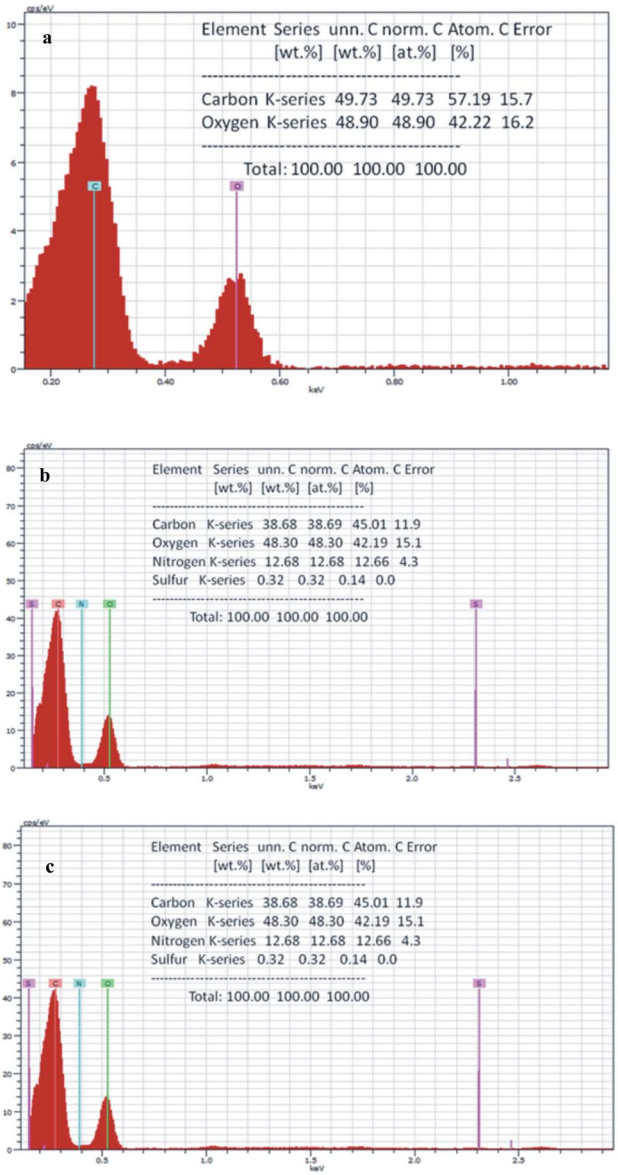

Fig. 5 EDS of (a) GO (b) In@GO NC and (c) In@GO NgC.

diameter and the size of GO NgC was 8.61 nm in diameter, while the diameter of Ng was 9.293 nm in PBS buffer (pH 7.4). Here it is worth mentioning that fabricated gels are not only biocompatible, but their controlled size also confirms the excretion of maximum GO *via* the urinary tract after delivery of insulin. The studies carried out to study the excretion of GO from the body after drug delivery found that GO sheets in the range of 8 nm can be excreted within 24 h *via* the urinary tract.[40]

The morphology of GO, In@GO NC and In@GO NgC was studied *via* SEM. Fig. 4a shows layers of exfoliated GO; however, they are thicker with fewer interlayer spaces. In contrast, Fig. 4b shows that due to intercalation these layers are separated and the interlayer spaces are increased. The SEM image of In@GO NgC shows that the synthesized gel is porous in nature (Fig. 4c).

The elemental analysis of the materials was performed through EDS. The results show that the GO contains (Fig. 5a) 57.19% carbon and 42.22% oxygen, while in the case of In@GO NC (Fig. 5b), the percentage of carbon and oxygen is decreased to 45.53% and 40.10%, respectively, and the addition of nitrogen (13.83%) and sulfur (0.54%) is evident due to the presence of insulin. The EDS of In@GO NgC (Fig. 5c) shows the same four elements such as carbon 45.01%, oxygen 42.19%, nitrogen 12.66% and sulfur 0.14%. The oxygen contents are increased in In@GO NgC due to the presence of HEMA and NIPAM.[41,42]

Physical and thermodynamic properties of materials were assessed by a differential scanning calorimetric instrument (Mettler Toledo 822e equipment). Fig. 6a shows the DSC of GO. In the DSC curve of GO, an irreversible broad endothermic peak is observed in the range of 4 to 9 minutes that corresponds to 65 to 115 °C. This peak is due to the elimination of entrapped water molecules between the exfoliated layers of GO. The prominent exothermic peak at 225 °C is observed in GO due to reduction of GO. The exothermic peak is prominently modified and appears at 215 °C with reduced intensity in DSC curve of In@GO NC (Fig. 6b). The reduced intensity of peak shows that the presence of intercalated insulin has altered the reduction of GO by providing the protection to oxygen functionalities of GO.[43]

The swelling study of synthesized nanogels in different pH mediums was performed (Table 1). The results obtained by the swelling study at different pH values revealed that In@GO NgC has a higher degree of swelling as well as the swelling ratio at pH 6.8 and 7.4 which makes it suitable for the effective delivery and absorption of insulin as more release is expected at intestinal pH. Moreover, the swelling degree is reduced incredibly at pH 1.2 which is also helpful for preventing release of insulin in the stomach as release in the stomach decreases bioavailability of drug. It can also be observed that at all the pH values In@GO NgC show a greater swelling degree as compared to GO NgC and nanogel (Table 1).

The relative viscosity of synthesized nanogels was calculated by the formula:

$$\eta 1/\eta 2 = \rho 1 t 1/\rho 2 t 2$$

It is found as 1.52 poise, 1.51 poise and 1.46 poise for In@GO NgC, GO NgC, and Ng, respectively. The viscosity of nanogels

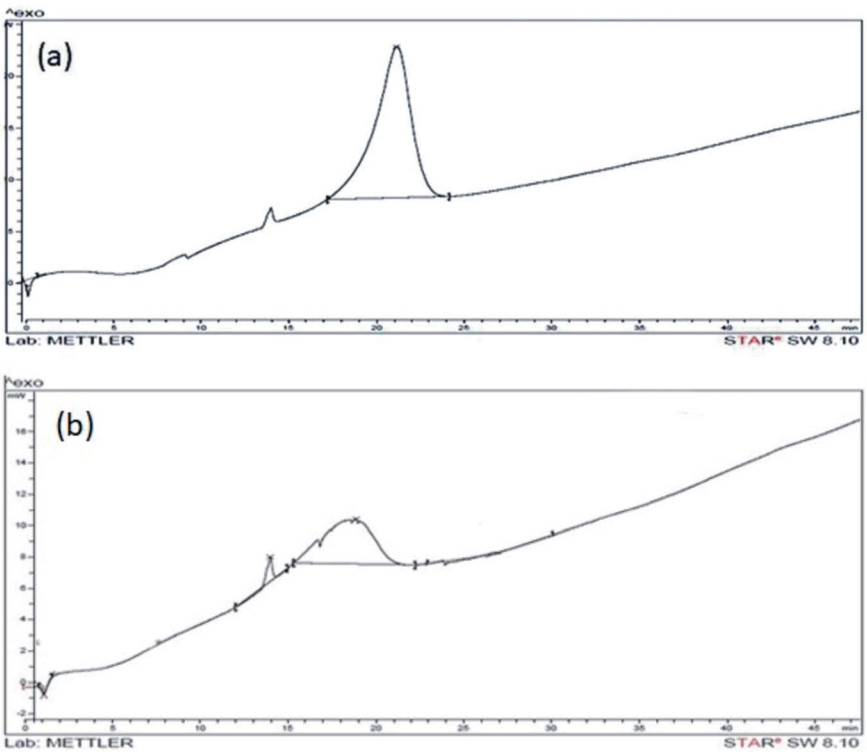

Fig. 6 DSC of (a) GO and (b) In@GO NC.

Table 1 Swelling study of nanogels in different pH mediums

		In@GO NgC		GO NgC		Ng	
S. no.	Medium pH	Swelling degree	Swelling ratio (%)	Swelling degree	Swelling ratio (%)	Swelling degree	Swelling ratio (%)
1	DI	0.03 ± 0.01	2.92 ± 0.21	0.03 ± 0.01	0.21 ± 0.1	0.02 ± 0.001	0.11 ± 0.1
2	6.8	11.63 ± 0.09	92.1 ± 0.13	6.34 ± 0.09	62.02 ± 0.12	2.32 ± 0.09	22.02 ± 0.12
3	7.5	7.35 ± 0.23	88.03 ± 0.11	4.05 ± 0.23	58.03 ± 0.11	1.03 ± 0.23	18.03 ± 0.11
4	1.2	0.95 ± 0.02	48.79 ± 0.05	0.23 ± 0.02	28.79 ± 0.05	0.03 ± 0.02	4.79 ± 0.05

Table 2 Loading efficiency of nanogels

Nanogel	M_1 (mg)	M_t (mg)	% LE
In@GO NgC	45	50	90
GO NgC	30	50	60
Ng	10	50	20

was increased due to interaction of GO and In@GO NgC with a polymeric backbone.

Loading efficiency of In@GO NgC was found as 90%, however, GO NgC and Ng showed 60% and 20% loading efficiency, respectively (Table 2). In@GO NgC has shown the highest loading efficiency because of the prior intercalation method, the insulin molecule was intercalated in between the layers of graphene oxide due to which the interlayer spaces are increased as much as the size of an insulin molecule. At the time of loading of insulin, the In@GO NgC gives a better loading efficiency. Moreover, intercalation of insulin during fabrication of In@GO NgC allowed the GO sheets to arrange themselves according to the interactions between GO and insulin. After completion of polymerization the intercalated insulin was denatured and removed. However, In@GO NgC was left with insulin specific interlayer spaces and arrangements that were ready to rebind insulin molecule again specifically. Hence, here the intercalation process produced the templating effect that is responsible for greater loading of insulin as compared to other nanogels.

In vitro release studies of insulin

The release of insulin was evaluated using synthesized nanogels in artificial gastric and intestinal fluids (Fig. 7). The release profile of insulin in artificial gastric fluid (pH 1.2) indicates that In@GO NgC shows the least release of insulin as compared to GO NgC and Ng. In gastric fluid (pH 1.2), an initial burst release of insulin was found as 29%, 33% and 46% using In@GO NgC, GO NgC and Ng, respectively. However, in the intestinal fluid (pH 7.5) the release profile of insulin was characterised by a significant initial burst in the first hour along with continuous and controlled release for the next 6 hours. The initial burst release of insulin in intestinal fluid was found as 57.66%, 53.89% and 41.89% using In@GO NgC, GO NgC and Ng, respectively. Better release of insulin was observed in artificial intestinal fluid as compared to artificial gastric fluid using In@GO NgC because in artificial gastric fluid the ion

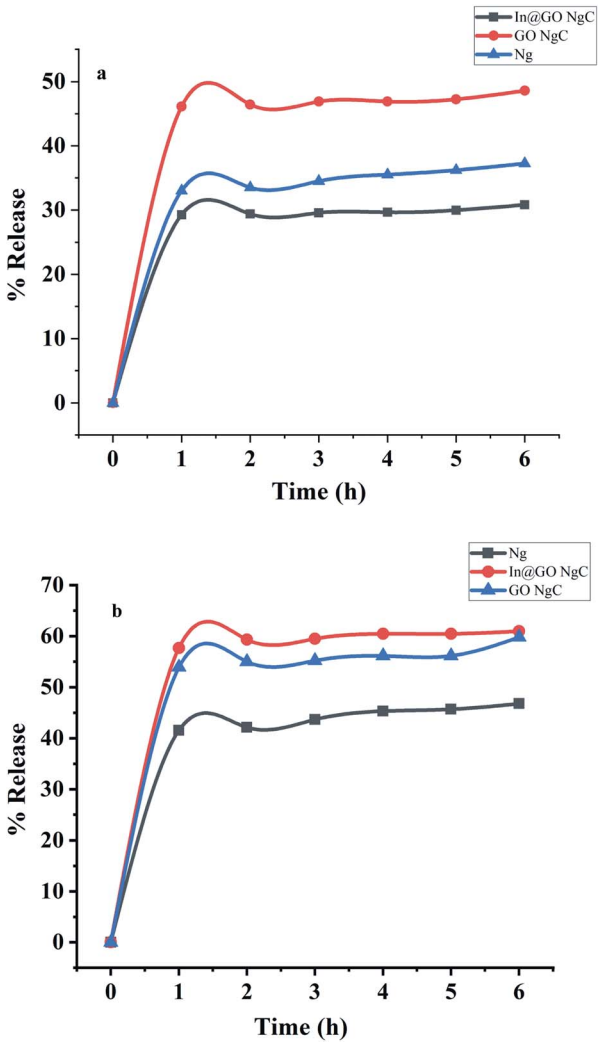

Fig. 7 *In vitro* release of insulin towards (a) artificial gastric fluid and (b) artificial intestinal fluid.

exchangers caused microsphere erosion and therefore more insulin was released. The In@GO NgC shows better release as compared to GO NgC and Ng. Intercalation of insulin with graphene oxide gives better release at intestinal pH.[44] Along with the biocompatibility of graphene oxide, HEMA and NIPAAM are also biocompatible, biodegradable and stimulant responsive materials.[25,31,39]

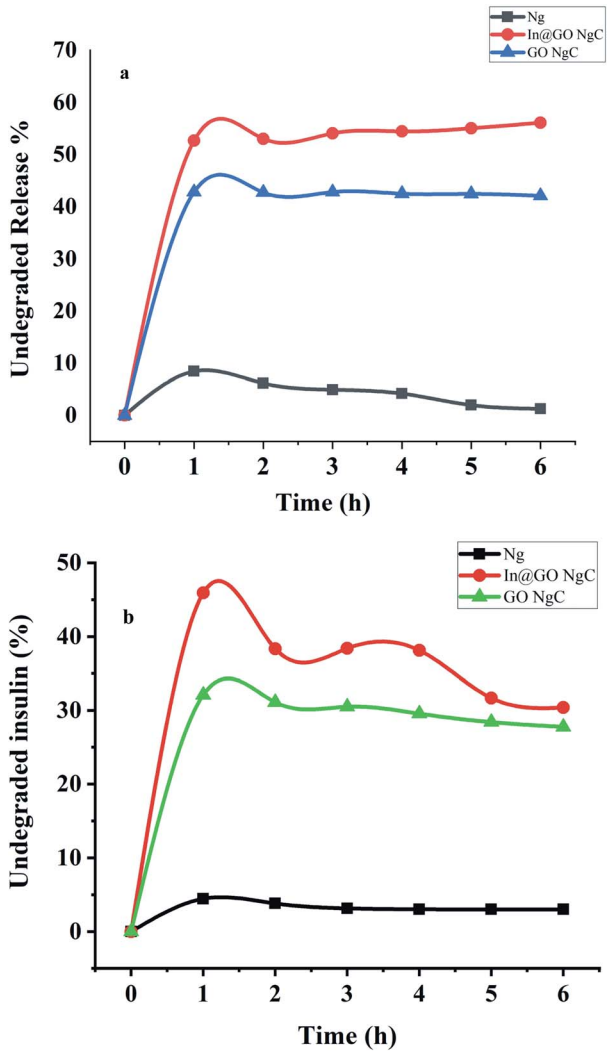

Fig. 8 *In vitro* release of insulin towards (a) artificial gastric fluid with pepsin and (b) artificial intestinal fluid with trypsin.

In vitro insulin release towards enzymatic fluids

The synthesized nanogels were tested for insulin degradation in the presence of enzymes after release. The concentrations of the enzymatic solutions were according to normal physiological conditions as shown in Fig. 8a and b. In artificial gastric fluid with pepsin, 56.14% undegraded insulin remains in In@GO NgC, 42.09% in GO NgC, and 1.28% undegraded insulin remains in Ng. While the results of intestinal fluid containing trypsin showed that 30.39% undegraded insulin remained in In@GO NgC, 27.78% in GO NgC and 3.01% un-degraded insulin remained in Ng. The degradation experiment was carried out for 6 hours.[45]

These results clearly indicate that the presence of GO in In@GO NgC and GO NgC prevents the degradation of insulin due to enzymatic fluids. It acts as a shield towards the enzymatic effect of pepsin and trypsin. However, Ng degrades completely and almost all of the insulin is degraded. These results confirm that the presence of GO in the structure of nanogels provides structural strength and toughness to face enzymatic degradation by interlocking nanogels into its interlayers.[31]

Drug-release-kinetics

The *in vitro* release of the insulin drug was examined by using various kinetic models (*i.e.*, zero order, first order, Higuchi, Korsmeyer–Peppas and Hixson–Crowell models). The constants of drug release (k, r, and n) have been calculated and it is found that all the three nanogels give a higher value of (r). Release of the insulin drug from the polymeric nanogels depends on the swelling solutions (buffers). The liquid moves into the nanogels, the drug gets dissolved in it, and the buffer moves out of the nanogels and swelling occurs.[46]

By application of the Higuchi model, the calculated value of (r) shows that the drug release pattern was diffusion controlled. The plot was designed in between the amount of drug released and the square root of time. However, the value of (n) for the insulin release was calculated by plotting the graph between the slope and intercept using the Korsmeyer–Peppas model. The value of n was in between 0.45 and 1, for all the three formulations at pH 7.5. It shows that the mechanism of diffusion existed as non-Fickian by polymeric swelling. The results show that the *in vitro* release of the drug for the nanogels at gastric pH 1.2 and intestinal pH 7.5 was well described by the Higuchi equation for drug release. The results showed higher linearity as displayed in Table 3. However, the values suggest that the drug release from nanogels was time dependent and the process of diffusion follows Fick's law.

Conclusions

In this study, the synthesis of nanogels was accomplished by the emulsion polymerization method for delivery of insulin.

Table 3 Release kinetics of drugs at different pH values from nanogels

S. no.	Nanogel	pH	Zero order kinetic model R^2	First order kinetic model R^2	Higuchi kinetic model R^2	Korsmeyer–Peppas model R^2	Hixson–Crowell model R^2
1	IN@GO NgC	1.2	0.994	0.997	0.931	0.994	0.999
		7.5	0.993	0.963	0.906	0.999	0.977
2	GO NgC	1.2	0.996	0.999	0.938	0.999	0.998
		7.5	0.997	0.976	0.903	0.999	0.985
3	Ng	1.2	0.986	0.958	0.883	0.997	0.969
		7.5	0.991	0.999	0.922	0.998	0.991

In@GO NgC appears technologically to be a promising delivery system for insulin. The nanogels were characterized thoroughly by different analytical techniques. The drug loading and release pattern of the synthesized nanogels at different physiological conditions revealed that In@GO NgC has a better loading efficiency and release at intestinal conditions. This is useful for greater absorption of insulin by the human body. Furthermore In@GO NgC is more stable towards enzymatic degradation. The Zetasizer results showed that introduction of In@GO into the nanogel did not affect its surface area and the size of the DDS. In fact, it provided it with stability and the controlled size of In@GO NgC such as 11.10 nm also confirmed that GO will not accumulate into body after delivery of insulin.

Author contributions

Shabana Gul Baloch mainly contributed to data curation, formal analysis, investigation and developing methodology. She also contributed to writing the manuscript. Huma Shaikh conceptualized, visualized and supervised the research work presented in this paper. She administered all the experiments and contributed to writing the original draft and revised and edited the manuscript. Shahnila Shah also contributed to data curation and manuscript writing. Shahabuddin Memon and Ayaz Ali Memon contributed to conceptualization and visualization of this research work. They also helped in the investigation during the experiments.

Conflicts of interest

There are no conflicts of interest to declare.

References

1 X. Zhao, X. Zou and L. Ye, Controlled pH- and glucose-responsive drug release behavior of cationic chitosan based nano-composite hydrogels by using graphene oxide as drug nanocarrier, *J. Ind. Eng. Chem.*, 2017, **49**, 36–45.
2 Z. Gu, *et al.*, Injectable nano-network for glucose-mediated insulin delivery, *ACS Nano*, 2013, **7**(5), 4194–4201.
3 I. D. Federation and I. D. J. I. D. F. Atlas, Brussels, 2013.
4 R. Langer, Drug delivery and targeting, *Nature*, 1998, 5–10.
5 J. Kost and R. Langer, Responsive polymer systems for controlled delivery of therapeutics, *Trends Biotechnol.*, 1992, **10**, 127–131.
6 M. Berger, H. Cüppers, H. Hegner, V. Jörgens and P. Berchtold, Absorption kinetics and biologic effects of subcutaneously injected insulin preparations, *Diabetes Care*, 1982, **5**(2), 77–91.
7 S. Yaturu, Insulin therapies: current and future trends at dawn, *World Journal of Diabetes*, 2013, **4**(1), 1.
8 V. Akbari, *et al.*, Efficacy and safety of oral insulin compared to subcutaneous insulin: a systematic review and meta-analysis, *J. Endocrinol. Invest.*, 2016, **39**(2), 215–225.
9 M. Lopes, S. Simões, F. Veiga, R. Seiça and A. Ribeiro, Why most oral insulin formulations do not reach clinical trials, *Ther. Delivery*, 2015, **6**(8), 973–987.
10 X. Chen, W. Wu, Z. Guo, J. Xin and J. Li, Controlled insulin release from glucose-sensitive self-assembled multilayer films based on 21-arm star polymer, *Biomaterials*, 2011, **32**(6), 1759–1766.
11 H. Von Bibra, W. Paulus, M. S. J. Sutton, C. Leclerque, T. Schuster and P.-M. Schumm-Draeger, Quantification of diastolic dysfunction via the age dependence of diastolic function—impact of insulin resistance with and without type 2 diabetes, *Int. J. Cardiol.*, 2015, **182**, 368–374.
12 O. Awoniyi, R. Rehman and S. Dagogo-Jack, Hypoglycemia in patients with type 1 diabetes: epidemiology, pathogenesis, and prevention, *Curr. Diabetes Rep.*, 2013, **13**(5), 669–678.
13 L. Zhang, Z. Gao, X. Zhao and G. Qi, A natural lipopeptide of surfactin for oral delivery of insulin, *Drug Delivery*, 2016, **23**(6), 2084–2093.
14 L. A. Klumb and T. A. Horbett, Design of insulin delivery devices based on glucose sensitive membranes, *J. Controlled Release*, 1992, **18**(1), 59–80.
15 K. Ishihara and K. Matsui, Glucose-responsive insulin release from polymer capsule1, *J. Polym. Sci., Part C: Polym. Lett.*, 1986, **24**(8), 413–417.
16 P. Hari, T. Chandy and C. P. Sharma, Chitosan/calcium alginate microcapsules for intestinal delivery of nitrofurantoin, *J. Microencapsulation*, 1996, **13**(3), 319–329.
17 M. Huguet and E. Dellacherie, Calcium alginate beads coated with chitosan: effect of the structure of encapsulated materials on their release, *Process Biochem.*, 1996, **31**(8), 745–751.
18 A. Rubinstein, *et al.*, The rationale for peptide drug delivery to the colon and the potential of polymeric carriers as effective tools, *J. Controlled Release*, 1997, **46**(1–2), 59–73.
19 A. Maroni, L. Zema, M. D. Del Curto, A. Foppoli and A. Gazzaniga, Oral colon delivery of insulin with the aid of functional adjuvants, *Adv. Drug Delivery Rev.*, 2012, **64**(6), 540–556.
20 M. Krzywon, T. van der Burg, U. Fuhr, M. Schubert-Zsilavecz and M. Abdel-Tawab, Study on the dosing accuracy of commonly used disposable insulin pens, *Diabetes Technol. Ther.*, 2012, **14**(9), 804–809.
21 R. B. Shah, M. Patel, D. M. Maahs and V. N. Shah, Insulin delivery methods: Past, present and future, *Int. J. Pharm. Invest.*, 2016, **6**(1), 1.
22 K. Akiyoshi, S. Deguchi, N. Moriguchi, S. Yamaguchi and J. Sunamoto, Self-aggregates of hydrophobized polysaccharides in water. Formation and characteristics of nanoparticles, *Macromolecules*, 1993, **26**(12), 3062–3068.
23 S. V. J. S. Vinogradov and f. p. o. c. systems, *16 Hydrophilic Colloidal Networks (Micro- and Nanogels) in Drug Delivery and Diagnostics*, 2009, vol. 146, p. 367.
24 A. V. Kabanov and S. V. Vinogradov, Nanogels as pharmaceutical carriers: finite networks of infinite capabilities, *Angew. Chem., Int. Ed.*, 2009, **48**(30), 5418–5429.
25 X. Wang, D. Cheng, L. Liu and X. Li, Development of poly(hydroxyethyl methacrylate) nanogel for effective oral insulin delivery, *Pharm. Dev. Technol.*, 2018, **23**(4), 351–357.

26 T. Hoare and R. Pelton, Engineering glucose swelling responses in poly(*N*-isopropylacrylamide)-based microgels, *Macromolecules*, 2007, **40**(3), 670–678.
27 W. F. Lee and Y. T. Fu, Effect of montmorillonite on the swelling behavior and drug-release behavior of nanocomposite hydrogels, *J. Appl. Polym. Sci.*, 2003, **89**(13), 3652–3660.
28 X. Yang, X. Zhang, Y. Ma, Y. Huang, Y. Wang and Y. Chen, Superparamagnetic graphene oxide–Fe_3O_4 nanoparticles hybrid for controlled targeted drug carriers, *J. Mater. Chem.*, 2009, **19**(18), 2710–2714.
29 Z. Liu, J. T. Robinson, X. Sun and H. Dai, PEGylated nanographene oxide for delivery of water-insoluble cancer drugs, *J. Am. Chem. Soc.*, 2008, **130**(33), 10876–10877.
30 L. Shahriary and A. A. Athawale, Graphene oxide synthesized by using modified Hummer's approach, *International Journal of Renewable Energy and Environmental Engineering*, 2014, **2**(01), 58–63.
31 S. Önal and F. Zihniğlu, Encapsulation of insulin in chitosan-coated alginate beads: oral therapeutic peptide delivery, *Artif. Cells, Blood Substitutes, Biotechnol.*, 2002, **30**(3), 229–237.
32 S. Dash, P. N. Murthy, L. Nath and P. Chowdhury, Kinetic modeling on drug release from controlled drug delivery systems, *Acta Pol. Pharm.*, 2010, **67**(3), 217–223.
33 N. Najib and M. S. Suleiman, The kinetics of drug release from ethylcellulose solid dispersions, *Drug Dev. Ind. Pharm.*, 1985, **11**(12), 2169–2181.
34 N. A. Peppas and B. Narasimhan, Mathematical models in drug delivery: How modeling has shaped the way we design new drug delivery systems, *J. Controlled Release*, 2014, **190**, 75–81.
35 T. Higuchi, Mechanism of sustained-action medication. Theoretical analysis of rate of release of solid drugs dispersed in solid matrices, *J. Pharm. Sci.*, 1963, **52**(12), 1145–1149.
36 K. Krishnamoorthy, M. Veerapandian, K. Yun and S.-J. Kim, The chemical and structural analysis of graphene oxide with different degrees of oxidation, *Carbon*, 2013, **53**, 38–49.
37 C. He, *et al.*, Chemically induced graft copolymerization of 2-hydroxyethyl methacrylate onto polyurethane surface for improving blood compatibility, *Appl. Surf. Sci.*, 2011, **258**(2), 755–760.
38 S. M. Rezaei and Z. M. Ishak, The biocompatibility and hydrophilicity evaluation of collagen grafted poly(dimethylsiloxane) and poly(2-hydroxyethylmethacrylate) blends, *Polym. Test.*, 2011, **30**(1), 69–75.
39 S. Sarkar, D. Das, P. Dutta, J. Kalita, S. B. Wann and P. Manna, Chitosan: A promising therapeutic agent and effective drug delivery system in managing diabetes mellitus, *Carbohydr. Polym.*, 2020, **247**, 116594.
40 D. A. Jasim, *et al.*, Thickness of functionalized graphene oxide sheets plays critical role in tissue accumulation and urinary excretion: a pilot PET/CT study, *Appl. Mater. Today*, 2016, **4**, 24–30.
41 F. Mindivan, The synthesis and characterization of graphene oxide (GO) and reduced graphene oxide (rGO), *Mach., Technol., Mater.*, 2016, **2**, 51–54.
42 Q. Bao, D. Zhang and P. Qi, Synthesis and characterization of silver nanoparticle and graphene oxide nanosheet composites as a bactericidal agent for water disinfection, *J. Colloid Interface Sci.*, 2011, **360**(2), 463–470.
43 V. Patil, R. V. Dennis, T. K. Rout, S. Banerjee and G. D. Yadav, Graphene oxide and functionalized multi walled carbon nanotubes as epoxy curing agents: a novel synthetic approach to nanocomposites containing active nanostructured fillers, *RSC Adv.*, 2014, **4**(90), 49264–49272.
44 M. Bakhshpour, H. Yavuz and A. Denizli, Controlled release of mitomycin C from PHEMAH–Cu(II) cryogel membranes, *Artif. Cells, Nanomed., Biotechnol.*, 2018, **46**(sup1), 946–954.
45 W. Yu, R. Liu, Y. Zhou and H. Gao, Size-tunable strategies for a tumor targeted drug delivery system, *ACS Cent. Sci.*, 2020, **6**(2), 100–116.
46 R. Gouda, H. Baishya and Z. Qing, Application of mathematical models in drug release kinetics of carbidopa and levodopa ER tablets, *J. Dev. Drugs*, 2017, **6**(02), 1–8.